THE JOURNAL OF PHYSICAL CHEMISTRY B

ARTICLE

pubs.acs.org/JPCB

Nanosecond Relaxation Dynamics of Hydrated Proteins: Water versus Protein Contributions

S. Khodadadi,*[,†] J. E. Curtis,[†] and A. P. Sokolov[‡]

[†]NIST Center for Neutron Research, National Institute of Standards and Technology, Gaithersburg, Maryland 20899, United States

[‡]Chemical Sciences Division, Oak Ridge National Laboratory, Oak Ridge, Tennessee 37831, United States, and Department of Chemistry, University of Tennessee, Knoxville, Tennessee 37996, United States

Supporting Information

ABSTRACT: We have studied picosecond to nanosecond dynamics of hydrated protein powders using dielectric spectroscopy and molecular dynamics (MD) simulations. Our analysis of hydrogen-atom single particle dynamics from MD simulations focused on "main" ($\tau_{main} \approx$ tens of picoseconds) and "slow" ($\tau_{slow} \approx$ nanosecond) relaxation processes that were observed in dielectric spectra of similar hydrated protein samples. Traditionally, the interpretation of these processes observed in dielectric spectra has been ascribed to the relaxation behavior of hydration water tightly bounded to a protein and not to protein atoms. Detailed analysis of the MD simulations and comparison to dielectric data indicate that the observed relaxation process in the nanosecond time range of hydrated protein spectra is mainly due to protein atoms. The relaxation processes involve the entire structure of protein including atoms in the protein backbone, side chains, and turns. Both surface and buried protein atoms contribute to the slow processes; however, surface atoms demonstrate slightly faster relaxation dynamics. Analysis of the water molecule residence and dipolar relaxation correlation behavior indicates that the hydration water relaxes at much shorter time scales.

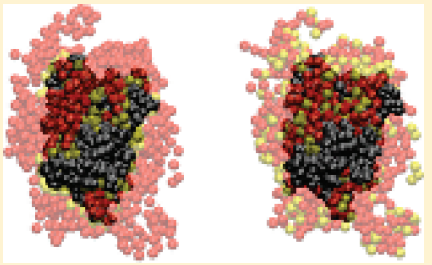

INTRODUCTION

Proteins and other biological macromolecules in physiological conditions are not frozen structures but fluctuate between various conformational states. In that respect, proteins resemble a liquid state of matter. Their internal dynamics span over an enormous frequency range and include several local and collective motions from bond vibrations and side group librations to larger-scale domain motions. Various NMR, neutron, and light scattering techniques, dielectric relaxation spectroscopy, and molecular dynamics (MD) simulations have been actively used to analyze protein, DNA, and RNA dynamics over broad frequency and temperature ranges. Yet, a general picture of the dynamics in biological macromolecules is absent.[1−22]

Neutron scattering studies and MD simulations have identified clearly four characteristic processes in protein dynamics on a time scale shorter than 1 ns at ambient temperature:[1−8] (i) low-frequency collective vibrations, similar to the boson peak in glass-forming systems; (ii) fast picosecond conformational fluctuations, that by analogy with similar fluctuations in glass-forming systems can be ascribed to a rattling of a residue in a cage formed by neighbor residues and solvent molecules; (iii) methyl group dynamics on a time scale of 15−30 ps, and (iv) slower relaxation process with the relaxation time $\tau \approx$ 25−50 ps that has been currently ascribed to a coupled protein−hydration water relaxation process.[5−8] The latter process has a strong temperature dependence and is the cause for the sharp rise of mean-squared atomic displacements with temperature above ≈220 K that is known as the dynamical transition in proteins.[6,7] NMR data usually present more site-specific information and reveal motions of many side group and backbone atoms on a time scale from ≈10 ps to ≈1 ns.[9,10]

Dielectric spectroscopy can be used to measure the relaxation spectra of protein solutions and hydrated protein powders with high accuracy over a very broad frequency range.[6,7,11,21,23] However, a significant disadvantage of dielectric spectroscopy is that the assignment of the measured relaxation modes to specific atomistic features is not possible because the technique measures motions of all the dipoles in the sample. It has been demonstrated that there are at least two relaxation processes in the dielectric spectra of aqueous protein solutions in the frequency range between protein tumbling (≈1−10 MHz) and bulk water relaxation (≈20 GHz).[10,11,21,23,24] The fastest relaxation process ($\tau \approx$ 20−50 ps) is usually ascribed to water of protein hydration that is slowed down, relative to the dynamics of bulk water, due to interactions with the protein.[10,11,21,23,24] However, even this assignment has been questioned recently.[6,7,23,24] The slower processes ($\tau \approx$ 0.5−10 ns) are traditionally ascribed to hydration water tightly bounded to a protein.[11,21,25] Many recent studies suggested that this process (or processes) can be ascribed either to protein relaxation,

Received: December 23, 2010
Revised: April 5, 2011
Published: April 22, 2011

including side groups and hinge-bending motions, or to the cross-term resulting from protein−water dipolar interactions.[6,7,11,23] The absence of clear assignments of the relaxation modes in dielectric spectra strongly limits the use of dielectric spectroscopy in the analysis of dynamics of biological macromolecules.

In this paper, we present detailed studies of dynamics of protein RNase A and its hydration shell with means of MD simulations. The results are compared to the previously published dielectric relaxation data of the proteins lysozyme[6,7,21] and RNase A.[21,24] The presented analysis reveals that there are very few hydration water molecules that do not exchange with bulk water on a time scale of 1 ns. Therefore, the dielectric relaxation process in the nanosecond time range cannot be ascribed to motions of hydration water, while protein atoms clearly exhibit relaxation processes in this time range. Our analysis concludes that protein atoms are the significant contributors to dynamical relaxation processes observed in hydrated proteins on the nanosecond time scale.

MATERIAL AND METHODS

Dielectric Relaxation Data. A detailed description of the sample preparation and dielectric measurements of lysozyme is presented in our earlier publication.[7] Therefore, herein a brief description of the methods will be presented. HEW lysozyme (Sigma-Aldrich) was dissolved in distilled water to 20 mg/mL and dialyzed for 48 h to remove salts. Protein was then lyophilized, and the dry protein powder was hydrated using isopiestic equilibration to obtain 0.4 g of water per gram of protein. Hydration levels were determined by thermogravimetric analysis. Dielectric spectra in the frequency range from 10^{-2} to 10^{7} Hz were measured using a Concept 80 system from Novocontrol. Samples were placed between two gold-coated parallel-plate electrodes, and a Teflon ring was used as a spacer. To prevent evaporation of water, an external Teflon ring was used to seal the samples. The capacitor formed with the sealed sample was placed in a cryostat. Temperature was stabilized to a precision of 0.1 K by using nitrogen gas flow and a Novocontrol Quatro temperature controller. Appropriate control measurements were performed twice to confirm the reproducibility of the measurements. Weighing the samples before and after data acquisition did not show any significant weight changes, indicating that hydration was kept constant during the measurements.

The real (ε') and imaginary (ε'') parts of the measured complex dielectric permittivity ε^* spectra of hydrated lysozyme at temperatures of 150−265 K were analyzed (Figure 1). In hydrated protein samples, the spectra of ε'' have several contributing factors: (a) a tail of conductivity at low frequencies, (b) a main relaxation process, and (c) another relaxation process that lies between the conductivity and main relaxation processes, a slow relaxation process that overlaps strongly with conductivity (Figure 1b). Conductivity does not contribute to the real part of permittivity, ε'. However, electrode polarization effects (due to accumulation of ions on electrodes) affect ε' at lower frequencies (Figure 1a). Still, ε' usually opens the possibility to study dielectric relaxation spectra at lower frequency than ε''. Thus, we used derivative analysis of the ε' (via Kramers−Kronig relationship) for estimates of the peak frequency of the slow process (Figure 1b)

$$\varepsilon'' \propto -\frac{2}{\pi}\frac{d\varepsilon'}{d\log\nu} \qquad (1)$$

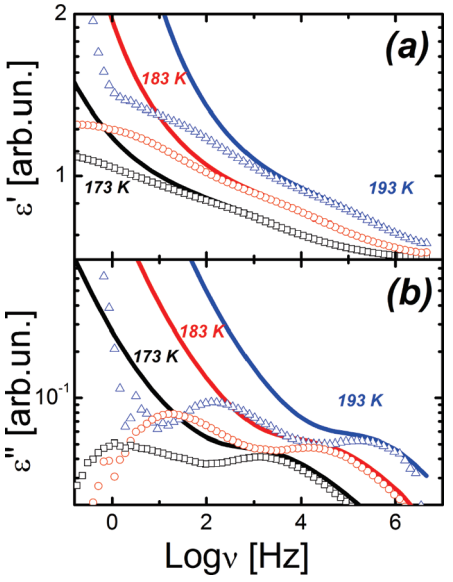

Figure 1. Dielectric spectra of the hydrated lysozyme ($h \approx 0.4$) at different temperatures. (a) ε' (solid lines) and after subtracting the electrode polarization effect (symbols). (b) ε'' (solid lines) and the derivative of the corrected ε', $-2d(\varepsilon' - \text{electrode polarization})/\pi d \log \upsilon$ (symbols). The derivative of ε' is similar to the loss spectrum but has no conductivity contribution that dominates ε'' spectra at lower frequencies.

where ν is frequency. The estimated peak frequencies were used as starting values of the final fit of real and imaginary parts. The spectra were fit by a sum of two Cole−Cole functions

$$\varepsilon^* = \varepsilon_\infty + \sum_j \frac{(\Delta\varepsilon)_j}{1+(i\omega\tau_j)^{\alpha_j}} - i\frac{\sigma}{\varepsilon_0\omega^s}, \quad j = 1,2,3 \qquad (2)$$

where $\omega = 2\pi\nu$ is angular frequency; τj is the relaxation time; $\Delta\varepsilon j$ is the dielectric strength; and αj is the stretching parameter of the j relaxation process. σ represents the amplitude of the conductivity tail, and s is the exponent describing the tail slope. We emphasize that we used the final fit of the real part of the permittivity spectra, corrected for the electrode polarization effect (subtracted a power law at low frequencies), to estimate the relaxation times and stretching parameters of the relaxation processes. Details of the fit procedure and data analysis can be found in our earlier publications.[6,7]

Molecular Dynamics Simulations. To analyze atomistic details of the protein motions, we performed MD simulations of the protein RNase A. This system has been used in previous studies, and it has been shown to quantitatively reproduce both water and protein dynamics as compared to neutron scattering data.[26−29] The computational results were derived from a 50 ns trajectory of RNase A in a hydrated crystal (2 RNase molecules plus 817 TIP3P waters[30]). The trajectory is a continuation of the simulation previously described.[31] The CHARMM-22 force field[31] was used as incorporated in the program PINY_MD.[32] The pre-equilibrated hydrated RNase A system was simulated at 300 K, 1 bar, for 50 ns in the NPT ensemble using periodic boundary conditions. Prior to analysis, each protein configuration at each time step was corrected for center of mass and rotational motion. Incoherent intermediate scattering functions were calculated as previously described.[26−29,33] We calculated water residence correlation functions, $<R(t)\cdot R(0)>/R(0)$, for water oxygen

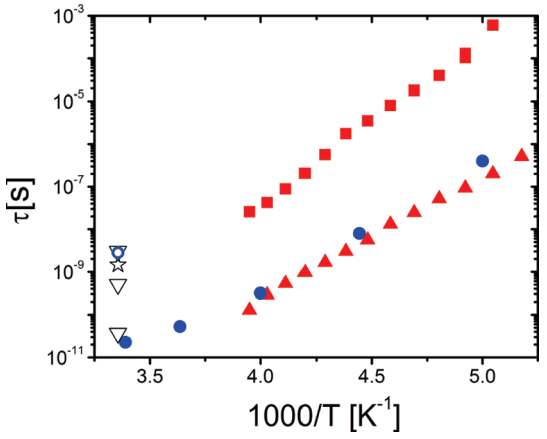

Figure 2. Temperature dependence of the relaxation times observed in hydrated proteins by dielectric spectroscopy. Hydrated lysozyme ($h \approx 0.4$) powder (data from ref 7): ▲, faster relaxation process; ■, slower relaxation process. Protein solutions at T = 298K: ▽, RNase A; ☆, RNase A; and ○, lysozyme (data from refs 21 and 24). ●, neutron scattering data for lysozyme relaxation in hydrated powder ($h \approx 0.4$, data from ref 7). Error bars for dielectric data are the size of symbols and represent the standard deviation.

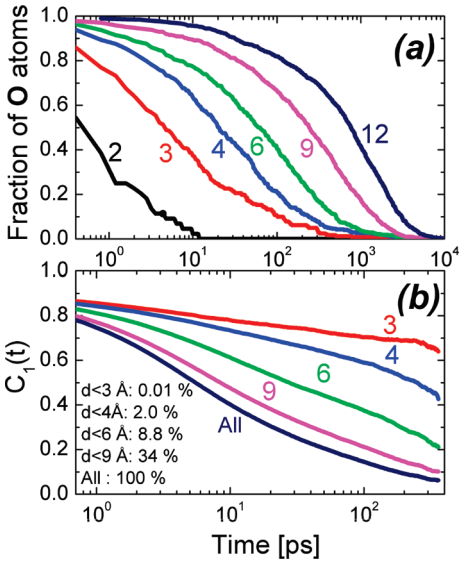

Figure 3. Residence relaxation and water dipolar correlation functions. (a) Time evolution of the fraction of water molecules that remain within a certain distance from the protein surface (R_{off}, in Å shown by numbers). (b) Orientational autocorrelation function of water molecules as a function of time. Cut-off distances and total water percentage for the given subset are shown in the figure. Correlation functions were calculated for a length of time such that a given population of water molecules that were present in a shell at an arbitrary initial time (t = 0) were still present in the same shell at 400 ps.

atoms as described previously.[34] $R(t)$ at the particular time t was judged to be either 1, when the water oxygen atom in question was within a predetermined cutoff distance, R_{off}, from the protein surface, or 0, when the distance was greater than R_{off}. If a water oxygen atom moved a distance greater than R_{off}, it was not counted in subsequent time steps. Orientational autocorrelation time of water, $C_1(t)$, was calculated from $\langle \boldsymbol{\mu}_i(t) \cdot \boldsymbol{\mu}_i(0) \rangle / |\boldsymbol{\mu}_i(0)|$ for waters that remained within a given distance cutoff criterion for the length of time used to calculate the correlation function. This correlation function corresponds to the average of the Legendre polynomial, $P_1(\cos(\Theta_i(t))$, for each water molecule and represents the molecular contribution measured by dielectric spectroscopy.[35]

RESULTS AND DISCUSSION

Figure 1 shows examples of dielectric relaxation spectra of hydrated lysozyme. Unfortunately, ionic conductivity dominates the dielectric loss spectra ε'' at lower frequencies and masks low frequency relaxation processes. One of the ways to visualize the spectra is to use a derivative of the real part of the dielectric permittivity ε' that, according to the Kramers−Kronig relationship, reflects the loss spectrum. Conductivity does not contribute to ε', and lower frequencies become accessible (a detailed discussion of this approach has been previously presented in ref 7), although one should be aware of electrode polarization effects and some additional artifacts related to ionic conductivity that might appear in both ε' and ε'' as a Debye-like relaxation process.[36] These analyses clearly show two strong relaxation processes in hydrated lysozyme (Figure 1). Both processes are strongly stretched and are comprised of elements with nearly equal areas. The latter aspect indicates that the relaxation strength of both processes (i.e., total fluctuations of the dipole moment of the structural units involved in these modes) is similar. We notice that the data exhibit a slight decrease in amplitude of the processes as temperature decreases, while usually an opposite variation is expected. This effect is more pronounced for the slower process. The observed behavior could be due to a real effect caused by slight compression of the sample with cooling, some broadening of the relaxation spectra, and an increase in separation between the relaxation peaks upon cooling. However, we cannot exclude that a part of the effect in the case of the slower process could be caused by interference with electrode polarization and its correction.

Temperature dependence of the relaxation times of the observed processes is shown in Figure 2. The dielectric relaxation times of hydrated lysozyme were shown only at temperatures below 253 K because the faster process moves out of the accessible frequency window at higher temperatures. Both processes exhibit strong temperature dependence, as shown in Figure 2. Earlier neutron scattering data[6,7] have revealed a relaxation process in hydrated proteins and are shown for comparison purposes in Figure 2. The relaxation time and temperature dependence agree well with $\tau(T)$ of the faster dielectric process. In addition, we include in Figure 2 literature data for the dielectric relaxation times measured in dilute aqueous solutions of lysozyme and RNase A at ambient temperature.[21,24] Although the data for dilute solutions do not overlap with the data for lysozyme in hydrated powder (Figure 2), the results clearly suggest that the same processes are observed in the dielectric relaxation spectra of hydrated powders and dilute solutions.

Figure 3a shows the fraction of water molecules that remain at a variety of cutoff distances from protein surface atoms. The majority of water molecules at a distance ≈3−4 Å from the protein surface (larger than the size of a water molecule) exchange with bulk water on the time scale less than 100 ps. Water dipole relaxation data are shown in Figure 3b, and relaxation data-fitting parameters can be found in the Supporting Information. The dipolar correlation function was calculated for

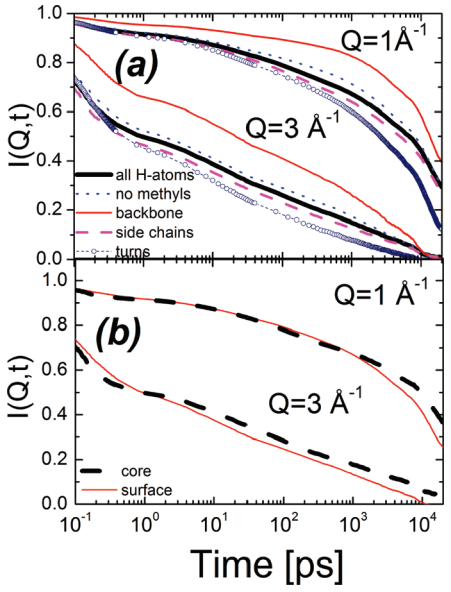

Figure 4. Intermediate scattering function of hydrogen atoms in RNase A at two selected scattering wave vectors Q: (a) Thick solid lines, all H-atoms; dotted lines, all H-atoms but methyl groups are excluded; thin solid lines, backbone H-atoms; dashed lines, side chain H-atoms; symbol + dashed lines, H-atoms in turns. (b) Intermediate scattering function of H-atoms in RNase A separated for core residues (thick dashed lines) and for surface residues (thin solid lines).

only those water molecules that remained within the given cutoff distance for the 400 ps time frame of the calculation. It was found that, on average, less than 0.1% of waters have dipolar relaxation times greater than 1 ns.

The calculated incoherent intermediate scattering function, $I(Q,t)$, of protein hydrogen atoms exhibits three processes shown in Figure 4 ($I(Q,t)$ data-fitting parameters can be found in Supporting Information). These relaxation steps involve (1) a fast relaxation on a time scale faster than 1 ps; (2) a very broad relaxation process on a time scale ≈10−30 ps which is better visible at higher Q; and (3) a slower process on a time scale ≈1−10 ns. The amplitude of these processes depends strongly on Q and the part of the molecule analyzed (e.g., backbone versus side chains). It has been reported that the dynamics of methyl group protons significantly contributes to dynamics of protein hydrogen atoms.[19,37]

Our analysis suggests that the exclusion of methyl hydrogen atoms does not significantly affect the behavior of $I(Q,t)$ in the present conditions. The contribution of methyl group dynamics is usually important at lower temperature or in dehydrated proteins, where other dynamic processes are strongly suppressed.

We focus our analysis on two relaxation processes visible in both dielectric spectra and in the incoherent intermediate scattering function obtained from MD simulations (Figures 1, 2, and 4(a)). The process around 10−30 ps is very broad and appears clearly in $I(Q,t)$ only at higher Q. This indicates that this process is spatially local. Earlier studies of the neutron scattering data of proteins hydrated in D_2O indicate that this process involves the motion of protein atoms confined to a space within radius ≈3 Å.[37] It is apparent that all parts of the protein, side chains, backbone, and especially turns are involved in this process, consistent with previous simulation reports of protein dynamics.[38,39] However, the motion of the backbone is significantly smaller than the motion of side chains and turns. This process in dielectric relaxation spectra is traditionally assigned solely to protein hydration water.[21,24,25] Indeed, analysis of hydration water indicates that it exchanges with the bulk on the time scale ≈10−30 ps (Figure 3). However, proteins also exhibit clearly relaxation processes at the same time scale (Figures 2 and 4). Thus, we assign this process to coupled water−protein motions.

The slower relaxation process observed in the nanosecond time range also involves all parts of the protein, although it seems that hydrogen atoms in turns relax faster than in the protein backbone (Figure 4(a)). The significant amplitude of this process even at Q = 1 Å^{-1} suggests that a large amplitude of the atomic motions is involved in this process. The analysis of incoherent intermediate scattering function data unambiguously assigns this process to protein motion. Also recent neutron spin−echo studies have revealed large coherent domain motions in protein Alcohol Dehydrogenase (ADH) on the time scale of ≈30 ns.[40] The longer characteristic time in this case might be related to the significantly larger size of the protein ADH or the inclusion of collective motions not analyzed in the MD simulations discussed herein.

However, the process that appears at the same time scale in dielectric relaxation spectra is usually ascribed to motion of water molecules tightly bounded to the protein,[11,21] although this assignment has been questioned.[7,23,24] Analysis of the dielectric relaxation spectra reveals that the amplitude of this process is comparable to the amplitude of the faster process as seen in Figure 1 and reported in the literature.[24] This observation suggests that the total dipole moment should be large to significantly contribute to the nanosecond relaxation process. It cannot be only attributed to a few water molecules. Additionally, MD simulations (Figure 3) clearly indicate that most of the hydration water molecules (water molecules on a distance ≈2−6 Å from the protein surface) exchange with the bulk on a time scale shorter than 1 ns and that >99.9% of the water molecules have predicted dipolar relaxation times less than 1 ns. Even if only a few protein hydration water molecules do not exchange with the bulk on this time scale, they would not significantly contribute to the dielectric signal. Thus, the analysis of the simulation results (Figure 3 and 4(a)) leads to a clear conclusion—the relaxation process at the nanosecond time scale is associated mostly with internal protein dynamics. However, the MD simulations were performed using classical force-fields with nonpolarizable, fixed partial charges, and the magnitude of the contribution due to mutual protein−water dipolar interactions on the relaxation process is not known. Therefore, one cannot exclude the possibility that this process in dielectric spectra can be at least partially influenced by a protein−water cross-term in dielectric relaxation.[23,24,41] We also want to mention a recent idea presented in refs 42 and 43 where the authors ascribed a part of the dielectric response to motion of water continuum (not individual molecules) caused by motions of the protein surface.

It is known that the dipole moment in proteins accumulates along α-helix secondary structure elements,[44] and the motion of this accumulated dipole will be much slower than the motion of dipoles of individual residues. Thus, it is probable that motions of secondary structure contribute to the relaxation process on the nanosecond time scale. To get better insight into the microscopic origin of this relaxation process in proteins, we separately analyzed the incoherent intermediate scattering function of surface residues and of the protein core (Figure 4(b)). The analysis clearly shows that both the surface and the core of the

protein are involved in this relaxation. The surface atoms, however, exhibit slightly faster relaxation processes.

CONCLUSIONS

Combined analysis of MD simulations and of the dielectric relaxation spectra of hydrated proteins clearly demonstrates that the relaxation process observed in the nanosecond time range cannot be assigned only to hydration water. Protein hydration water exchanges with the bulk water on a time scale faster than 100 ps. Simulations, as well as literature neutron scattering data, reveal unambiguously the presence of protein relaxation in the nanosecond time range. This relaxation involves the entire protein, including backbone, side chains and turns, surface, and the core of the protein, although the surface residues seem to exhibit faster dynamics. We speculate that this process might be connected with motions of secondary structures of the protein. However, details of the contribution of different segments and secondary structure of the protein motions at the nanosecond time scale remain unclear.

ASSOCIATED CONTENT

Supporting Information. Figures S1−S3 and Tables S1−S9. This material is available free of charge via the Internet at http://pubs.acs.org.

AUTHOR INFORMATION

Corresponding Author
*E-mail: sheila.khodadadi@nist.gov.

ACKNOWLEDGMENT

We acknowledge the partial financial support from NSF (DMR-1059562). S.K. acknowledges the National Research Council for support. Certain commercial equipment, instruments, materials, suppliers, or software are identified in this paper to foster understanding. Such identification does not imply recommendation or endorsement by the National Institute of Standards and Technology, nor does it imply that the materials or equipment identified are necessarily the best available for the purpose.

REFERENCES

(1) Sokolov, A. P.; Gregory, R. B. *Neutron Scattering in Biology-Techniques and Applications*; Springer: New York, 2005.
(2) Parak, F. G. *Rep. Prog. Phys.* **2003**, *66*, 103–129.
(3) Tarek, M.; Tobias, D. J. *J. Chem. Phys.* **2001**, *115*, 1607–1612.
(4) Bengtzelius, W.; Götze, W.; Sjölander, A. *J. Phys. (Paris)* **1984**, *C17*, 5915–5933.
(5) Gabel, F.; Bicout, D.; Lehnert, U.; Tehei, M.; Weik, M.; Zaccai, G. *Q. Rev. Biophys.* **2002**, *35*, 327–367.
(6) Khodadadi., S.; Pawlus, S.; Roh, J. H.; V. Garcia Sakai, V.; Mamontov, E.; Sokolov, A. P. *J. Chem. Phys.* **2008**, *128*, 195106/1–195106/5.
(7) Khodadadi, S.; Pawlus, S.; Sokolov, A. P. *J. Phys. Chem. B* **2008**, *112*, 14273–14280.
(8) Doster, W.; Settle, M. *Biochim. Biophys. Acta* **2005**, *1749*, 173–186.
(9) Buck, M.; Boyd, J.; Redfield, C.; MacKenzie, D. A.; Jeenes, D. J.; Archer, D. B.; Dobson, C. M. *Biochemistry* **1995**, *34*, 4041–4055.
(10) Krushelnitsky, A.; Reichert, D. *Prog. Nucl. Magn. Reson. Spectrosc.* **2005**, *47*, 1–25.
(11) Hayashi, Y.; Miura, N.; Isobe, J.; Shinyashiki, N; Yagihara, S. *Biophys. J.* **2000**, *79*, 1023–1029.
(12) Götze, W.; Sjögren, L. *J. Phys. (Paris)* **1987**, *C20*, 879–894.
(13) Götze, W.; Sjögren, L. *J. Phys. (Paris)* **1988**, *C21*, 3407–3471.
(14) Doster, W.; Settles, M. *Workshop on Hydration Processes in Biology: Theoretical and Experimental Approaches*; Bellissent-Funel, M. C., Ed.; IOS Press: Les Houches, 1998; pp 177−191.
(15) Doster, W.; Cusack, S.; Petry, W. *Nature* **1989**, *337*, 754–756.
(16) Caliskan, G.; Kisliuk, A.; Sokolov, A. P. *J. Non-Cryst. Solids* **2002**, *307−310*, 868–873.
(17) Caliskan, G.; Kisliuk, A.; Tsai, A.; Soles, C.; Sokolov, A. P. *J. Chem. Phys.* **2003**, *118*, 4230–4236.
(18) Tournier, A. L.; Smith, J. C. *Phys. Rev. Lett.* **2003**, *91*, 208106/1–208106/4.
(19) Roh, J. H.; Novikov, V. N.; Gregory, R. B.; Curtis, J. E.; Chowdhuri, Z.; Sokolov, A. P. *Phys. Rev. Lett.* **2005**, *95*, 038101/1–038101/4.
(20) Krishnan, M.; Kurkal-Siebert, V.; Smith, J. C. *J. Phys. Chem. B* **2008**, *112*, 5522–5533.
(21) Miura, N.; Asaka, N.; Shinyashiki, N; Mashimo, S. *Biopolymers* **1994**, *34*, 357–364.
(22) Gregory, R. B.; Gangoda, M.; Gilpin, R. K.; Su, W. *Biopolymers* **1993**, *33*, 513–519.
(23) Oleinikova, A.; Smolin, N.; Brovchenko, I. *Biophys. J.* **2007**, *93*, 2986–3000.
(24) Oleinikova, A.; Sasisanker, P.; Weingartner, H. *J. Phys. Chem. B* **2004**, *108*, 8467–8474.
(25) Jansson, H.; Bergman, R.; Swenson, J. *J. Phys. Chem. B* **2005**, *109*, 24134–24141.
(26) Tarek, M.; Tobias, D. J. *J. Am. Chem. Soc.* **2000**, *122*, 10450–10451.
(27) Tarek, M.; Tobias, D. J. *J. Am. Chem. Soc.* **1999**, *121*, 9740–9741.
(28) Tarek, M.; Tobias, D. J. *Biophys. J.* **2000**, *79*, 3244–3257.
(29) Tarek, M.; Tobias, D. J.; Curtis, J. E. *J. Am. Chem. Soc.* **2004**, *126*, 15928–15929.
(30) Stillinger, F. H.; A. Rahman, A. *J. Chem. Phys.* **1974**, *60*, 1545–1557.
(31) MacKerell., A. D., Jr.; Bashford, D.; Bellott, M.; Dunbrack., R. L., Jr.; Evanseck, J. M.; Field, M. J.; Fischer, S.; Gao, J.; Guo, H.; Ha, S.; Joseph-McCarthy, D.; Kuchnir, L.; Kuczera, K.; Lau, F. T. K.; Mattos, C.; Michnick, S.; Ngo, T.; Nguyen, D. T.; Prodhom, B.; Reiher, W. E.; Roux, B., III; Schlenkrich, M.; Smith, J. C.; Stote, R.; Straub, J.; Watanabe, M.; Wiorkiewicz-Kuczera, J.; Yin, D.; Karplus., M. *J. Phys. Chem. B* **1998**, *102*, 3586–3616.
(32) Tuckerman, M. E.; Yarne, D. A.; Samuleson, S. O.; Hughes, A. L.; Martyna, G. J. *Comput. Phys. Commun.* **2000**, *128*, 333–376.
(33) Dirama, T. E.; Curtis, J. E.; Carri, G. A. *J. Chem. Phys.* **2006**, *124*, 034901.
(34) Curtis, J. E.; Dirma, T.; Carri, G.; Tobias, G. *J. Phys. Chem. B* **2006**, *110*, 22953–22956.
(35) Kumar, P.; Franzese, G.; Buldyrev, S. V.; Stanley, H. E. *Phys. Rev. E* **2006**, *73*, 041505/1–041505/8.
(36) Richert, R.; Agapov, A.; Sokolov, A. P. *J. Chem. Phys.* **2011**, *134*, 104508.
(37) Roh, J. H.; Curtis, J. E.; Azzam, S.; Novikov, V. N.; Peral, I.; Chowdhuri, Z.; Gregory, R. B.; Sokolov, A. P. *Biophys. J.* **2006**, *91*, 2573–2588.
(38) McCammon, J. A.; Gellin, B. R.; Karplus, M. *Nature* **1977**, *267*, 585–590.
(39) Arcangeli, C.; Bizzarri, A. R.; Cannistraro, S. *Chem. Phys. Lett.* **1998**, *291*, 7–14.
(40) Biehl, R.; Hoffmann, B.; Monkenbusch, M.; Falus, P.; Preost, S.; Merkel, R.; Richter, D. *Phys. Rev. Lett.* **2008**, *101*, 138102/1–138102/4.
(41) Nandi, N.; Bhattacharyya, K.; Bagchi, B. *Chem. Rev.* **2000**, *100*, 2013–2045.
(42) LeBard, D. N.; Matyushov, D. V. *J. Phys. Chem. B* **2008**, *112*, 5218–5227.
(43) Matyushov, D. V.; Morozov, A. Y. arXiv: 1011.1023.
(44) Sengupta, D.; Behera, R. N.; Smith, J. C.; Ullmann, G. M. *Structure* **2005**, *13*, 849–855.